Supplementary Material to:

12 May 2008 M=7.9 Wenchuan, China, earthquake calculated to increase failure stress and seismicity rate on three major fault systems

by Shinji Toda, Jian Lin, Mustapha Meghraoui, and Ross S. Stein

Methodology and parameter assumptions.

1) Coulomb stress change in an elastic half space.

This discussion abstracts material from *Toda and Stein* [2003] and *Toda et al* [2005] and then applies it to the Wenchuan earthquake source and receiver faults and the associated ISC earthquake catalog. The static Coulomb stress change ΔCFF caused by a main shock is calculated by

$$\Delta CFF = \Delta\tau + \mu' \Delta\sigma_n \qquad (1)$$

where $\Delta\tau$ is the shear stress change on a given fault plane (positive in the direction of fault slip), $\Delta\sigma_n$ is the fault-normal stress change (positive when unclamped), and μ' is the effective coefficient of friction which precludes distinguishuing the effect of pore pressure change from the normal stress change (clamping/unclamping). We make all calculations in an elastc half-space [*Okada*, 1992] in which deformation is controlled by Poisson's ratio (0.25) and shear modulus (3.2 x 10^5 bars).

In Fig. 1, we compute stress tensors brought from the deformation produced by the variable slip models composed of 22 x 5 patches by *Ji and Hayes* [2008] and 21 x 8 patches by *Nishimura and Yagi* [2008]. The coseismic Couomb stress change at each gridded node is resolved in the fault slip direction defined at the node based on smoothed version of strike, dip, and rake assumed from local structural control shown in at a right-bottom corner of Fig. 1a. The mapped stress changes in Fig. 1 are represented at a depth of 10 km, which is roughly at mid-depth of the seismogenic layer. Apparent coefficient of friction used in Fig. 1 is set to be 0.4 to minimize the uncertainty [*King et al*., 2004] for a representative figure. We also calculated the stress changes for the likely range of the effective coefficient of 0.0-0.8 and depths between 5-15 km (Fig. S1). The calculated 0.2-0.3 bar stress increase along 250 km of the Kunlun fault, as well as the 0.2-0.5 bar increase within the 1893 and 1955 rupture zones of the Xianshuihe fault between Daofu and Kangding, are evident in all cases. In contrast, the stress increase extending southwest of the mainshock rupture, and the increase north of Chengdu in the Sichuan basin, are sensitive to friction.

Coulomb stresses are also resolved along plausible slip directions (rake) and dips on the major active faults listed in Table 1 and Fig. 1. Since the nucleation process for a large rupture [Dieterich, 1994] tends to start from the most active off-fault aftershock zones where the stress change is likely to be maximized, we identify the largest Coulomb stress increase along a fault from the combination of the seismogenic depth range of 10-15 km and apparent friction ranges of 0.0-0.8 (column 10 in Table 1).

2) Rate- and state stress transfer model.

To translate coseismic stress changes associated with the Wenchuan mainshock into the expected rate of seismicity and thus probability, we use the expression for seismicity rate R as a function of the state variable γ under a tectonic secular shear stressing rate $\dot{\tau}_r$ from *Dieterich* [1994]. Under constant shear stressing rate, the state variable γ reaches the steady state, and is expressed as

$$\gamma_0 = \frac{1}{\dot{\tau}_r} \tag{2}$$

At steady state, the seismicity rate R is equivalent to the background rate (also called the reference rate) r because R is calculated from the following relation

$$R = \frac{r}{\gamma \dot{\tau}_r} \tag{3}$$

In the absence of a stress perturbation, the seismicity rate is assumed constant. We index the state variable γ with time. If an earthquake strikes, it imposes a sudden stress step ΔCFF, and the state variable before the step γ_{n-1} changes to a new state value γ_n

$$\gamma_n = \gamma_{n-1} \exp\left(\frac{-\Delta CFF}{A\sigma}\right) \tag{4}$$

where $A\sigma$ is a constitutive parameter times the effective normal stress, assumed here to be a range of 0.1 and 0.5 bars based on the previous studies [*Toda and Stein*, 2003; *Catalli et al.*, 2008]. To seek the seismicity at the time of the stress step, we substitute the new state variable in (4). In rate/state friction there is a nonlinear dependence of the time to instability on stress change. A stress increase on a fault causes γ to drop, so the fault slips at a higher rate, yielding a higher rate of seismicity. Conversely, a sudden stress drop causes γ to jump, lowering the rate of seismicity. The seismicity rate change is transient and eventually recovers, corresponding to a gradual evolution of

γ, which for the next time step Δt is given by

$$\gamma_{n+1} = \left[\gamma_n - \frac{1}{\dot{\tau}_r}\right]\exp\left[\frac{-\Delta t \dot{\tau}_r}{A\sigma}\right] + \frac{1}{\dot{\tau}_r} \quad (5)$$

The duration of the transient defined t_a is expressed as

$$t_a = \frac{A\sigma}{\dot{\tau}_r} \quad , \quad (6)$$

which means t_a is inversely proportional to the fault-stressing rate $\dot{\tau}_r$ under the constant $A\sigma$. Given sufficient time (e.g., decades to centuries), the effect of all but the largest stress changes disappears except the one on the most slowly stressed faults (low $\dot{\tau}_r$). A key feature of rate/state stress transfer is that the value of γ before each shock plays a profound role on the effect of the stress change on seismicity: the higher the rate of seismicity at the time of a stress increase, the more strongly the seismicity rate will be amplified by the stress change. Further, the effect of each earthquake in a series continues to affect γ. Since we lack detailed fault source models for the past large earthquakes in and around the Longman Shan region, here we consider only the Wenchuan earthquake source.

To estimate the value of reference rate of seismicity r, one needs a stable earthquake catalog with the largest number of earthquakes above the completeness threshold. Since the seismic networks and seismometers tend to develop year by year, we first need to examine minimum magnitude of completeness (Mc) as a function of time (Fig. 2a) and then decide which period and Mc are appropriate for using spatial reference rate of regional seismicity. In this paper, we used ZMAP (*Wiemer*, 2001) that assumes that the magnitude where a simple regression line of Gutenberg-Richter relation departs from the observation represents Mc. Using the International Seimological Center (ISC, http://www.isc.ac.uk/) catalog in our study area, we found Mc = 3.2 during the period of 2000-January 2008. To make a spatial matrix of r, the catalog was smoothed with a 50-km-radius Gaussian filter for the earthquakes of M≥3.2 during the period and then normalized to the rates per 100 x 100 km^2 for 10 year (Fig. 2b).

To calculate the 10-yr forecast rate in space (Fig. 2c and Fig. S2), we first updated the sudden change in state variable γ with calculated *ΔCFF* in equation (4) and then γ at each small time bin following the decay or recovery process. Cumulative expected number of shocks in space is color-coded by integrating R based on γ for the entire 10-yr period between 2008 and 2017.

To estimate the seismicity rate change in column 11 of Table 1, we set $r = 1$ and then seek values of R/r with the parameter ranges of t_a and $A\sigma$.

3) Earthquake probability

To calculate 10-yr probabilities for earthquakes of M≥6.0 and M≥7.0 from the expected rate of M≥3.2 earthquakes in Fig. 2, we assume a magnitude-frequency b-value of 1.0 and simply extrapolate the rate of M≥3.2 earthquakes to the rates for M≥6.0 and M≥7.0 earthquakes. The rates at all the calculation nodes can be spatially integrated to have a total rate R of large earthquakes in the entire study area of Fig. 2 and Fig. S2. We then translated R into the stational Poissonian probability P with the following simple formula,

$$P = 1 - \exp(-R). \quad (7)$$

Supplementary figures.

Figure S1. Sensitivity of the calculated stress transfer to assumed fault friction and calculation depth. The source fault model is from *Ji and Hayes* [2008]. Explanation on the lines and symbols are as in Figure 1.

Figure S2. Expected rates of the M≥3.2 earthquakes calculated by rate/state stress transfer, and probabilities for the M≥6.0 and M≥7.0 earthquakes for the next 10 years within the entire 750 x 770 km map frame.

References

Catalli, F., M. Cocco, R. Console, and L. Chiaraluce (2008), Modeling seismicity rate changes during the 1997 Umbria-Marche sequence (central Italy) through a rate- and state-dependent model, submitted to *J. Geophys. Res*.

Dieterich, J. (1994), A constitutive law for rate of earthquake production and its application to earthquake clustering, *J. Geophys. Res.*, *99*, 2601-2618.

Ji, C., and G. Hayes (2008), Preliminary result of the May 12, 2008 Mw 7.9 eastern Sichuan, China earthquake, http://earthquake.usgs.gov/eqcenter/eqinthenews/2008/us2008ryan/finite_fault.php.

King, G. C. P., R. S. Stein, and J. Lin (1994), Static stress changes and the triggering of earthquakes, *Bull. Seismol. Soc. Am*., 84, 935-953.

Nishimura, N., and Y. Yagi (2008), Rupture process for May 12, 2008 Sichuan earthquake (preliminary result), http://www.geol.tsukuba.ac.jp/~nisimura/20080512/.

Okada, Y., Internal deformation due to shear and tensile faults in a half-space (1992), *Bull. Seismol. Soc. Am*., 82, 1018-1040.

Toda, S., and R. Stein (2003), Toggling of seismicity by the 1997 Kagoshima earthquake couplet: demonstration of time-dependent stress transfer, *J. Geophys. Res*., 108, B12, 2567, doi:10.1029/2003JB002527.

Toda, S., R. S. Stein, K. Richards-Dinger and S. Bozkurt (2005), Forecasting the evolution of seismicity in southern California: Animations built on earthquake stress transfer*, J. Geophys. Res.,* B05S16, doi:10.1029/2004JB003415.

Wiemer, S., A software package to analyse seismicity: ZMAP (2001), *Seismol. Res. Lett*., 72, 373-382.

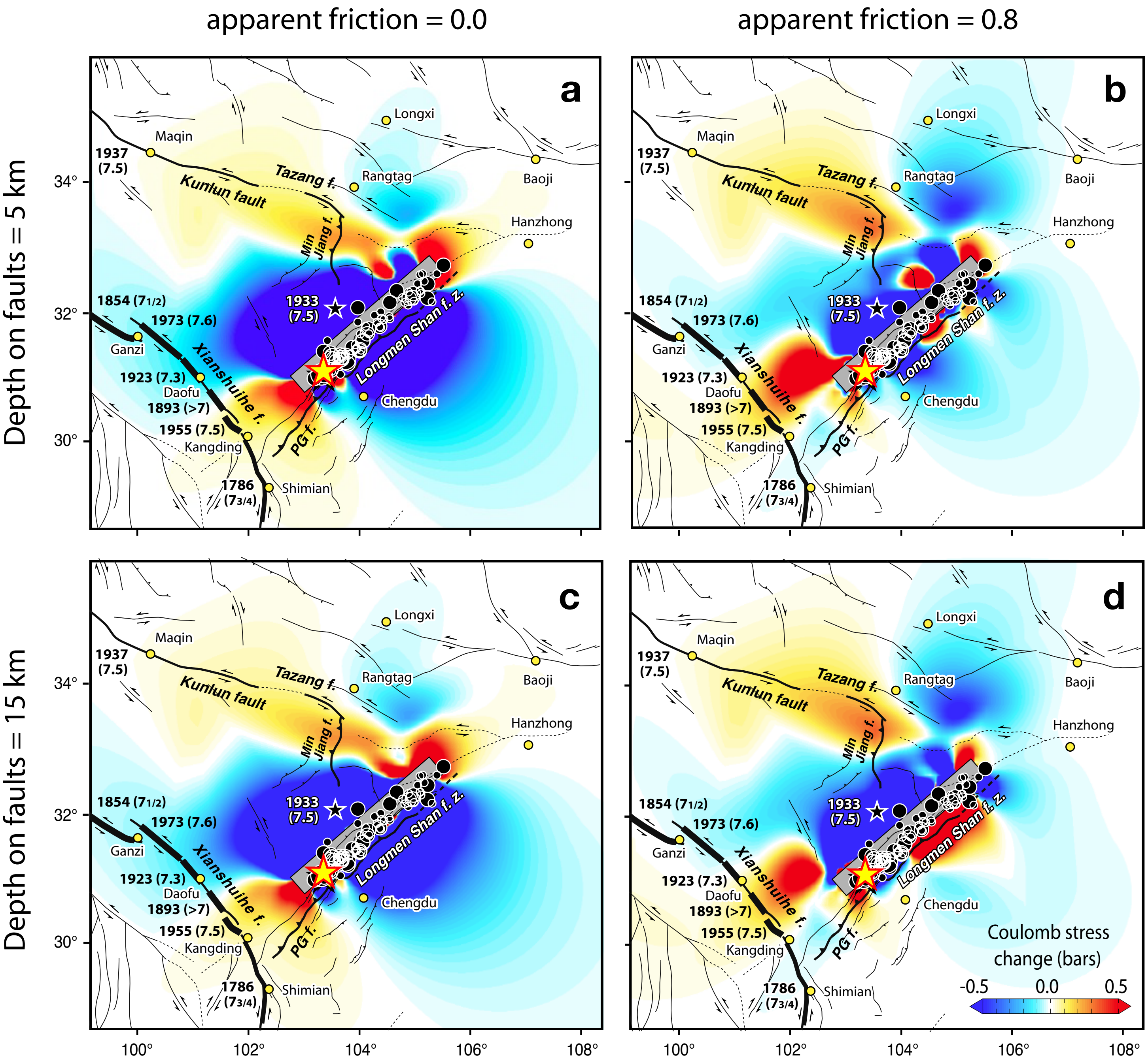

Fig. S1
Toda et al.

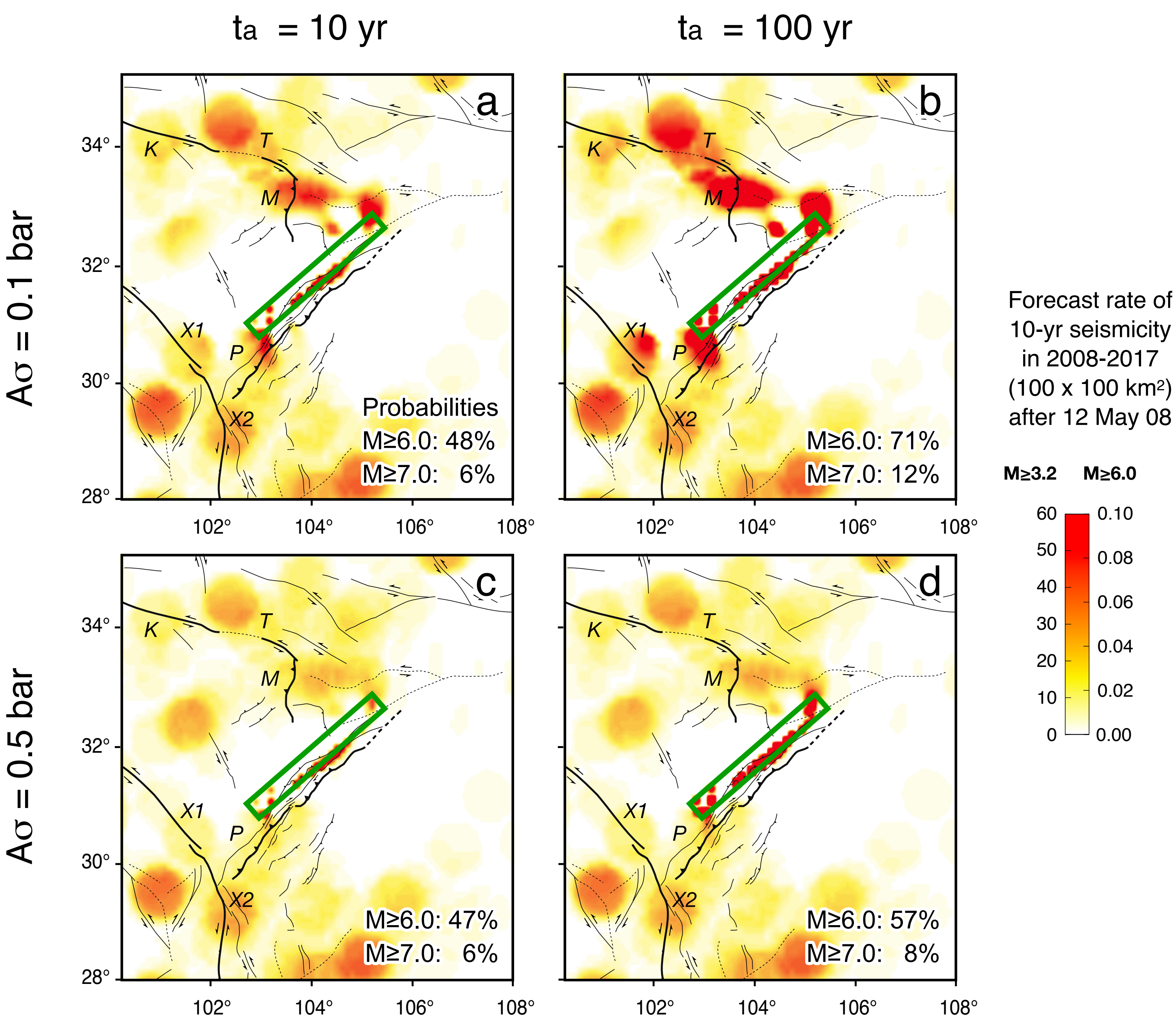

Fig. S2
Toda et al.